

DEVELOPMENT OF NANOCRYSTALLINE IRON-CHROMIUM ALLOY BY  
MEANS OF SINTERING AND ION IMPLANTATION FOR INTERCONNECT  
APPLICATION IN HIGH-TEMPERATURE SOLID OXIDE FUEL CELLS

DENI SHIDQI KHAERUDINI

A thesis is submitted in  
fulfilment of the requirements for the award of the  
Degree of Master in Mechanical Engineering

Faculty of Mechanical and Manufacturing Engineering  
Universiti Tun Hussein Onn Malaysia

NOVEMBER 2011

## ABSTRACT

This research is aimed to develop the nanocrystalline iron-chromium (FeCr) alloys by two different sintering methods, spark plasma sintering (SPS) and hot pressing (HP). The sintering temperatures in SPS are designed at 800 and 900 °C; meanwhile in HP at 1000 °C. The lower sintering temperature in SPS than HP was carried out in order to obtain the relatively similar in theoretical density of alloy with a minimum grain growth. The alloy has a potential application as interconnector in solid oxide fuel cell (SOFC). The beneficial effect of the reactive element by means of lanthanum (La) into the alloys surface which is introduced using ion implantation is also evaluated. The study focused on the properties, including thermal expansion, oxidation behaviour and electrical resistance of the surface oxide scales. Oxidation testing was conducted at 900-1100 °C for 100 h in laboratory air. Characterizations by using X-ray diffraction (XRD), scanning electron microscopy (SEM) and energy dispersive X-ray spectroscopy (EDS) were carried out before and after each route or process to investigate the microstructure, phase change, and formation of the oxide layer. The specific aspects studied were the effects of nanocrystalline structures, which influenced by the sintering method; and surface treatment through La ion implantation of chromia-forming alloys may improve their high thermal stability. The commercially available ferritic steel is chosen as the comparison with other high-Cr ferritic model alloys. The results revealed that the FeCr alloy prepared by SPS, to be more effective to retain nanocrystalline and better properties than those prepared by HP and commercially available ferritic steel. For all types of materials, the presence of La had no detectable effect on thermal expansion but a major effect on oxide scale adherence. The results consistently showed that better reduction in electrical resistance corresponds with excellent oxidation resistance of the alloy. The performance of FeCr alloy sintered by SPS and implanted by La exhibited the lowest oxidation and electrical resistance of the oxide scale.

## ABSTRAK

Penyelidikan ini bertujuan untuk membangunkan besi-kromium (FeCr) aloi *nanocrystalline* dengan dua kaedah pensinteran yang berbeza, *spark plasma sintering* (SPS) dan *hot pressing* (HP). Suhu pensinteran di SPS ditetapkan pada 800 dan 900 °C; sementara itu, di HP adalah pada 1000 °C. Suhu pensinteran yang lebih rendah di SPS daripada HP telah digunakan dalam usaha untuk mendapatkan ketumpatan teori aloi yang hampir sama dengan pertumbuhan butiran yang minimum. Ianya mempunyai potensi aplikasi sebagai *interconnector* dalam sel bahan bakar oksida padu (SOFC). Kebaikan penggunaan unsur reaktif iaitu lanthanum (La) ke permukaan aloi yang diperkenalkan menggunakan kaedah implantasi ion juga dikaji. Kajian ini tertumpu kepada sifat bahan iaitu pengembangan haba, pengoksidaan dan penebatan elektrik pada lapisan permukaan oksida. Pengoksidaan ujian dilakukan pada 900-1100 °C selama 100 jam di ruang udara makmal. Spesimen teroksida ditentukan dengan menggunakan pembelauan sinar-X (XRD), mikroskop pengimbas elektron (SEM) dan tenaga penyebaran sinar-X spektroskopi (EDS) yang dilakukan sebelum dan selepas pada setiap proses untuk mengkaji mikrostruktur, perubahan fasa, dan pembentukan lapisan oksida. Aspek spesifik yang diteliti adalah kesan struktur *nanocrystalline* yang dipengaruhi oleh kaedah sintering; dan rawatan permukaan melalui implantasi ion La dimana ianya dapat meningkatkan sifat kestabilan haba yang tinggi. Keluli feritik komersial dipilih sebagai perbandingan dengan model aloi Cr feritik. Hasil kajian menunjukkan bahawa FeCr aloi menggunakan kaedah SPS lebih efektif dalam mengekalkan sifat *nanocrystalline* berbanding dari yang dihasilkan oleh HP dan keluli feritik komersial. Untuk semua jenis bahan, kehadiran La tidak memberi kesan pada pengembangan haba namun memberi kesan yang besar pada pengikatan oksida. Keputusan yang konsisten menunjukkan bahawa pengurangan rintangan elektrik selari dengan rintangan pengoksidaan pada aloi. Prestasi FeCr aloi yang disinter oleh SPS dan diimplan oleh La menunjukkan pengoksidaan dan rintangan elektrik yang terendah.

**CONTENTS**

<b>TITLE</b>	<b>i</b>
<b>DECLARATION</b>	<b>ii</b>
<b>DEDICATION</b>	<b>iii</b>
<b>ACKNOWLEDGEMENTS</b>	<b>iv</b>
<b>ABSTRACT</b>	<b>v</b>
<b>ABSTRAK</b>	<b>vi</b>
<b>CONTENTS</b>	<b>vii</b>
<b>LIST OF TABLES</b>	<b>xi</b>
<b>LIST OF FIGURES</b>	<b>xii</b>
<b>LIST OF SYMBOLS AND ABBREVIATIONS</b>	<b>xvi</b>
<b>LIST OF APPENDICES</b>	<b>xviii</b>
<b>CHAPTER 1 INTRODUCTION</b>	<b>1</b>
1.1 Background of Study	1
1.2 Problem Statement	5

1.3	Objectives of Study	5
1.4	Scopes of Study	6
<b>CHAPTER 2 LITERATURE REVIEW</b>		<b>7</b>
2.1	Solid Oxide Fuel Cell	7
2.2	Interconnect	9
2.3	Potential Interconnect Alloys	11
2.3.1	Iron-Chromium Alloys	12
2.3.2	Other Metallic Materials	15
2.4	Consolidation Processing Route	17
2.5	Sintering	19
2.6	Surface Treatments via Ion Implantation	24
2.7	Thermal Expansion	29
2.8	Oxidation Resistance	32
2.9	Electrical Resistance	37
<b>CHAPTER 3 METHODOLOGY</b>		<b>42</b>
3.1	Starting Materials	42
3.2	Consolidation of Metal Powders to Bulk Shapes	42

3.2.1	Hot Pressing	43
3.2.2	Spark Plasma Sintering	44
3.3	The as-received Commercial Ferritic Alloy	46
3.4	Ion implantation Process for Surface Treatment	46
3.4.1	Samples Preparation	46
3.4.2	Ion Dose	47
3.5	Thermal Expansion	47
3.6	Oxidation Kinetics	49
3.7	Electrical Resistivity	51
3.8	Phase and Microstructural Characterization	53
3.9	Density	54
3.10	Flowchart	55
<b>CHAPTER 4 RESULTS AND DISCUSSIONS</b>		<b>56</b>
4.1	The FeCr powder	56
4.2	Sintered FeCr	59
4.3	Crystallite Size	64
4.4	Density	65

4.5	Thermal Expansion	66
4.6	High Temperature Oxidation	70
4.7	Electrical Resistance	95
<b>CHAPTER 5 CONCLUSIONS AND RECOMMENDATIONS</b>		<b>98</b>
5.1	Conclusions	98
5.2	Recommendations	99
<b>REFERENCES</b>		<b>101</b>
<b>APPENDICES</b>		<b>110</b>
<b>VITA</b>		

**LIST OF TABLES**

2.1	Linear coefficient of thermal expansion for currently used SOFC materials	30
2.2	Linear coefficient of thermal expansion (measured in air) between 30 °C and 800 °C as well as between 30 °C and 1000 °C of interconnect materials for SOFC	31
3.1	The chemical composition of the main elements containing in the investigated commercially available ferritic alloy (wt%)	46
4.1	Crystallite size of the FeCr samples, as received powder and after the HP or SPS consolidation, and the as received commercial alloy by using Williamson-Hall Equation Method	64
4.2	Density of the bulk FeCr samples, after the HP or SPS consolidation and the as received commercial alloy by using Archimedes Method	65
4.3	CTE values of FeCr samples and as received commercial alloy	69
4.4	Parabolic rate constants ( $k_p$ ) for investigated alloys calculated from oxidation data	74
4.5	Electrical resistivity for the investigated alloys obtained from I-V curve measurements	95



**LIST OF FIGURES**

2.1	Typical SOFC single cell configuration	8
2.2	Schematic of a typical planar SOFC stack	9
2.3	Phase diagram of Fe-Cr system	13
2.4	The three steps of sintering	17
2.5	Powder metallurgy route	19
2.6	Schematic of the hot pressing technique	20
2.7	Structural changes accompanying the preparation of a sintered product	20
2.8	Basic configuration of a typical SPS system	21
2.9	A schematic drawing of the pulsed current that flows through powder particles	22
2.10	Comparison of the relative densities of the Ti specimen prepared by SPS and conventional HP sintering as a function of the sintering temperature	23
2.11	SEM fractured surface of the Ti specimen prepared (a) by SPS at 700 °C for 5 min and (b) by conventional HP sintering at 900 °C for 1 h	23
2.12	Schematic configuration of the ion implanter system	25
2.13	Areas of layer depth (thickness) of various surface modification and coating processes	26
2.14	Cyclic oxidation kinetics of the bare and cerium implanted AZ31 at 500°C in air	27
2.15	Weight gain vs. time curves of blank and yttrium-implanted 304 stainless steel during oxidation at 1000 °C in air	28
2.16	Plots of mass gain vs time during oxidation of blank and pre-treated GH128 alloys at 1000 °C in air	29
2.17	Different oxidation kinetics	34

2.18	Kinetics (for 100 h) of coated and uncoated Crofer 22 APU at 800 °C in air under atmospheric pressure	35
2.19	Cross sectional backscattered electron images of (a) uncoated, (b) Y/Co-coated and (c) Ce/Co-coated AISI-SAE 430 stainless steels oxidized for 1000 h	36
2.20	Temperature-dependence of area specific resistance for undoped and doped Fe–26Cr–1Mo alloy oxidized at 800 °C for 24 h in air where Pt electrode was used for measurement	40
3.1	Sintering profile in hot pressing process	44
3.2	Sintering profile in spark plasma sintering process	45
3.3	Schematic of Linseis D-8672-SELB dilatometer	48
3.4	Temperature profile used for dilatometer sintering curves	49
3.5	Schematic of thermal cycles applied in this study	51
3.6	Schematic for the resistivity measurement setup	52
3.7	Flowchart of the experiment	55
4.1	The SEM images of the as received mechanically-alloyed Fe-20 wt% Cr powder (a) × 200 magnification and (b) × 1000 magnification	57
4.2	EDS results of the as received mechanically-alloyed Fe-20 wt% Cr powder	57
4.3	The XRD results of the as received mechanically-alloyed Fe-20 wt% Cr powder	58
4.4	Hot pressed samples	59
4.5	Spark plasma sintered samples (a) FeCr with SPS sintered at 800 °C and (b) FeCr with SPS sintered at 900 °C	59
4.6	SEM images for the as consolidated (a) FeCr with SPS Sintered at 800 °C, (b) FeCr with SPS sintered at 900 °C, (c) FeCr with HP sintered at 1000 °C, and (d) the as received commercial alloys	60
4.7	XRD results for the as consolidated samples, (a) FeCr with SPS sintered at 800°C and (b) FeCr with HP sintered at 1000°C	62
4.8	XRD results for the as consolidated and as received samples, (a) FeCr with SPS sintered at 900°C and (b) the as received commercial alloys	63

4.9	Comparison of CTE values between implanted and unimplanted for (a) FeCr SPS800 and (b) FeCr HP1000 samples	67
4.10	Comparison of CTE values between implanted and unimplanted for (a) FeCr SPS900 and (b) commercial alloy samples	68
4.11	Mass gain as function of oxidation time for all the specimens during oxidation at 900 °C for 100 h in air	73
4.12	Mass gain as function of oxidation time for all the specimens during oxidation at 1000 °C for 100 h in air	73
4.13	Mass gain as function of oxidation time for all the specimens during oxidation at 1100 °C for 100 h in air	74
4.14	The XRD results for the implanted samples (a) SPS800, (b) SPS900, (c) HP1000, (d) commercial alloy oxidized at 900 °C	77
4.15	The XRD results for the unimplanted samples (a) SPS800, (b) SPS900, (c) HP1000, (d) commercial alloy oxidized at 900 °C	77
4.16	The XRD results for the implanted samples (a) SPS800, (b) SPS900, (c) HP1000, (d) commercial alloy oxidized at 1000 °C	78
4.17	The XRD results for the unimplanted samples (a) SPS800, (b) SPS900, (c) HP1000, (d) commercial alloy oxidized at 1000 °C	78
4.18	The XRD results for the implanted samples (a) SPS800, (b) SPS900, (c) HP1000, (d) commercial alloy oxidized at 1100 °C	79
4.19	The XRD results for the unimplanted samples (a) SPS800, (b) SPS900, (c) HP1000, (d) commercial alloy oxidized at 1100 °C	79
4.20	SEM Surface morphology of the implanted and unimplanted specimens (a) SPS800, (b ) SPS900, (c) HP1000, (d) commercial alloy after 100 h oxidation at 900 °C in air	81
4.21	SEM Surface morphology of the implanted and unimplanted specimens (a) SPS800, (b ) SPS900, (c) HP1000,	

	(d) commercial alloy after 100 h oxidation at 1000 °C in air	83
4.22	SEM Surface morphology of the implanted and unimplanted specimens (a) SPS800, (b ) SPS900, (c) HP1000, (d) commercial alloy after 100 h oxidation at 1100 °C in air	84
4.23	SEM cross section and EDS line scan of the elements for Implanted and unimplanted (a) SPS800 and (b) HP1000 alloy specimens after 100 h oxidation at 900 °C	87
4.24	SEM cross section and EDS line scan of the elements for Implanted and unimplanted (a) SPS900 and (b) commercial alloy specimens after 100 h oxidation at 900 °C	88
4.25	SEM cross section and EDS line scan of the elements for Implanted and unimplanted (a) SPS800 and (b) HP1000 alloy specimens after 100 h oxidation at 1000 °C	89
4.26	SEM cross section and EDS line scan of the elements for Implanted and unimplanted (a) SPS900 and (b) commercial alloy Specimens after 100 h oxidation at 1000 °C	90
4.27	SEM cross section and EDS line scan of the elements for implanted and unimplanted (a) SPS800 and (b) HP1000 alloy specimens after 100 h oxidation at 1100 °C	91
4.28	SEM cross section and EDS line scan of the elements for Implanted and unimplanted (a) SPS900 and (b) commercial alloy specimens after 100 h oxidation at 1100 °C	92
4.29	Calculated area-specific resistance (ASR) values of the implanted and unimplanted specimens after 100 h oxidation at 900 °C, 1000 °C, and 1100 °C in air	96

## LIST OF SYMBOLS AND ABBREVIATIONS

Ce	-	Cerium
Fe	-	Ferum/Iron
Cr	-	Chromium
FeCr	-	Iron-Chromium
Fe <sub>2</sub> O <sub>3</sub>	-	Iron Oxide
(Fe,Cr) <sub>2</sub> O <sub>3</sub>	-	Iron Chromium Oxide
Cr <sub>2</sub> O <sub>3</sub>	-	Chromium Oxide/Chromia
La <sub>2</sub> O <sub>3</sub>	-	Lanthanum Oxide
LaCrO <sub>3</sub>	-	Lanthanum Chromite
LaB <sub>6</sub>	-	Lanthanum Hexaboride
La	-	Lanthanum
Se	-	Selenium
Ti	-	Titanium
Y	-	Yttrium
ASR	-	Area Specific Resistance
At%	-	Atomic Percentage
CTE	-	Coefficient of Thermal Expansion
Commercial	-	The as-received commercial ferritic alloy
DC	-	Direct Current
EDS	-	Energy Dispersion X-ray spectroscopy
FWHM	-	Full Width at the Half Maximum
h	-	Hour
HP	-	Hot Pressing
HP1000	-	FeCr specimen as ho pressed at 1000 °C
ICDD	-	International Centre for Diffraction Data
PDF	-	powder diffraction file
RE	-	Reactive Element

SEM	-	Scanning Electron Microscope
SOFC	-	Solid Oxide Fuel Cell
SPS	-	Spark Plasma Sintering
SPS800	-	FeCr specimen as spark plasma sintered at 800 °C
SPS900	-	FeCr specimen as spark plasma sintered at 900 °C
Wt%	-	Weight Percentage
XRD	-	X-Ray Diffraction

**LIST OF APPENDICES**

A	Calculation of Crystallite Size by Williamson-Hall Equation Method	111
B	Calculation of Density by Archimedes Method	112
C	Electrical Current-Voltage (I-V) Plots	113
D	List of Publications	117

## CHAPTER 1

### INTRODUCTION

#### 1.1 Background of Study

For decades the energy situation in the world has become more and more critical. Conventional energy sources are not sufficient to meet the constantly expanding needs of humanity, so exploration of new energy sources seems to be a challenging task for the future. One possibility for the alternative to conventional energy conversion systems is fuel cell development. Fuel cells are generally regarded to be of central importance for the transformation to the so-called hydrogen economy. These devices offer the impressive potential of efficient generation of power using fuel such as hydrogen with essentially no environmentally harmful by-products. As such, fuel cells have been the focus of many recent research programs (Stover *et al.*, 1999; Wu & Liu, 2010; Zhu & Deevi, 2003a).

One of the most promising and attention fuel cell systems seems to be Solid Oxide Fuel Cell (SOFC) because of its potential for becoming an efficient and high energy-density power generation device (Quadackers *et al.*, 2003; Steele, 2001). SOFC development requires the combination of broad groups of different engineering branches. One of the tasks is to invent the most suitable materials for all SOFC components (e.g. anode, cathode, electrolyte and interconnector).

Solid oxides possess sufficiently high ionic conductivity at the elevated temperatures so that SOFC must operate at the temperature range of 800 - 1000 °C. The repetitions of single cells constitute the single stack. However, this structure requires also a mechanical support and a current collector between the different cells to provide a higher voltage and power in a serial connection. Both properties are



provided by the interconnector plate. The availability of a suitable material for the interconnector is of key importance for SOFC development. This component is normally a ceramic based material (lanthanum chromite) but there is research trying to develop new interconnector fabricated with metallic alloys (Stöver *et al.*, 1999; Tietz *et al.*, 2002). Metallic materials have the advantage of a higher electronic conductivity, lower cost and easier fabrication than ceramics (Quadackers *et al.*, 2003). However, the SOFC operating environment is harsh and many common metal alloys are not capable of performing adequately over extended periods. This is especially challenging because the interconnector is exposed to both oxidizing conditions at the cathode and reducing conditions at the anode. This has led to the search for a metal alloy with specific physical and mechanical properties and retains their strength (thermal stability) at the elevated temperatures that could be applied successfully as a fuel cell interconnects.

The metal alloys have long been considered as potential candidates for high temperature applications because their high strength to weight ratio. Among metal alloys in common use, Cr-based alloys and high Cr- ferritic based alloys seem to be the most promising metallic interconnector that forms protective  $\text{Cr}_2\text{O}_3$  layers upon oxidation at the elevated high temperatures in the air (Quadackers *et al.*, 2003). This is due to a rather slow growth rate and a proper electric conductivity of the oxide scale (Quadackers *et al.*, 2003). However, development of the particular ferritic based alloys is a relatively complicated task because the material needs to fulfil several requirements to be suitable as a SOFC interconnector, which sometimes can be even contrary. Based on the requirements in respect to oxidation resistance, the continued growth of oxide scale or oxidation kinetics below  $10^{-14} \text{ g}^2\text{cm}^{-4}\text{s}^{-1}$  is required, and a value below  $10^{-15} \text{ g}^2\text{cm}^{-4}\text{s}^{-1}$  would be ideal (Antepara *et al.*, 2005), which can lead to the increasing of electrical resistance or lead to the thermal expansion mismatch during thermal cycling in both oxidizing and reducing atmosphere. A large number of ferritic alloys are commercially available in a wide range of compositions; conversely, it seems that none of them can fulfil all requirements for the SOFC interconnector (Quadackers *et al.*, 2003). Therefore, new FeCr based alloys have recently been developed specifically for SOFC applications. These materials seem to be sufficiently good for most of the envisaged SOFC applications; however, it is still necessary to improve their composition to design

alloy, which possesses excellent properties during operation in SOFC relevant atmospheres.

This present study is, in essence, a discussion on designing a nanostructured alloy with tailored properties, entirely in the solid state from metal powder precursor. However, the problems arise immediately when trying to manufacture the alloy related to conventional consolidation process, such as in hot pressing (HP). Mainly, due to longer processing times and higher temperature conditions, some grain growth in the structure could not completely be eliminated. When thermal energy is applied to a powder compact, the compact is densified and the average grain size increased. The full-density compacts with retaining nanometric grain size (nanostructured alloy), is of essential significance in interconnector SOFC application, which can produce better properties of alloys, specifically in the reduction the kinetics of oxidation and not easy to achieve. Therefore, in this work the mechanical alloyed Fe-Cr powder had been introduced using spark plasma sintering (SPS) technique to produce the bulk FeCr alloy, since this process is capable of control of producing many metallic alloys with a perfectly controlled degree of densification and microstructure with near theoretical density over 99 % at relatively lower sintering temperature (200 to 500 °C) than temperature used in conventional HP process (Omori, 2000). In spite of that, this method also cost effective sintering and can be completed in a short period of approximately 5 to 20 minutes including temperature rise and holding times (Omori, 2000). In particular, it is essential to compare these two sintering process, SPS and HP, in order to demonstrate the effectiveness of these approaches in improving the high temperature properties of the sintered alloy which would be of significant in practical importance, specifically in SOFC interconnector.

The use of controlled surface modification is a viable alternative to reduce oxidation rates and extend the useful life of a potential alloy as interconnects in SOFC. Ion implantation is a physical method for the modification of surface properties of materials by insertion of accelerated atoms, within the first atomic layers into solid substrates (Marest, 1998). As a process, ion implantation is widely used to modify the oxidation behaviour to the surface of the alloys. Modification of the corrosion behaviour of metal surfaces by ion implantation will allow the introducing of a controlled reactive element (RE) concentration into the alloys surface. It has been known that the minor addition of RE, such as La, Y, Ti, Hf, and Ce, could significantly improve the spallation resistance of these oxide scales under

oxidising and/or reducing conditions and inhibits further by isothermal and thermal cycling oxidation (Cooper *et al.*, 2008). This implantation on the surfaces of the Fe-Cr alloys may help mitigate chromium volatility, reduce the oxide scale growth rate of the chromia-forming alloy which can lead to the formation of phase that may increase the electrical resistance or lead to the thermal expansion mismatch during thermal cycling. In this research, the investigation, the beneficial effect of La ion implantation on the oxidation behaviour of alloys also is considered.

The main emphasis of this study was made to investigate the effect of each process in the high temperature oxidation resistance in the temperature range required for SOFC application (800 - 1000 °C). The scale formation mechanisms in the case of the most promising materials were investigated during oxidation times up to 100 hours and the influence of minor RE addition, specifically La, through surface treatment - ion implantation in the alloy was also elaborated. For a better understanding of the mechanisms of oxidation for Fe-Cr alloy, the available high-Cr ferritic model alloys were prepared and incorporated into the test program. Characterisations by using X-ray diffraction (XRD), scanning electron microscopy (SEM) and energy dispersive X-ray spectroscopy (EDS) was carried out to investigate the microstructure, phase change, and formation of the oxide layer. The electrical conductivity of the interconnector is a crucial property for SOFC application whereby the conductivity of the chromia based oxide scale formed on the metallic surface during stack operation has to be taken into account in the overall conductivity value. Nevertheless, the thermally grown oxide scale of the alloy may overgrow during operating temperature, resulting in scale spallation due to the thermal stress may occur in the alloys, which induced by the thermal expansion mismatch between the scale and substrate. Due to these issues, dilatometry studies were conducted to observe the thermal expansion behaviour of metal alloys which predict these values as a function of temperature is also the very important fundamental parameter in SOFC application.

## 1.2 Problem Statement

The identification and fabrication of suitable interconnector materials are a major challenge in the development of SOFC. Iron-Chromium or FeCr alloys have received considerable attention as potential interconnector materials due to high strength and thermal stability. However, the problems arise immediately when trying to manufacture the nanostructured FeCr alloy whereby steps must be taken to avoid the grain growth during solidification, which can influence to the improved properties of alloys, specifically in oxidation resistance and this is not easy to achieve. Thus, the temperature and time of consolidation have to be restricted at low value to keep the nanostructures by using the advance consolidation process - spark plasma sintering with respect to microstructural and smaller grain size control. On the other hand, they may fail through loss of strength or gradually deteriorate with the surrounding atmosphere during SOFC operating temperature. Therefore, the formation of a stable oxide layer through ion implantation is required to protect the underlying materials.

## 1.3 Objectives of Study

The main objective of the present work is to develop the nanostructured FeCr alloy using sintering and ion implantation for SOFC temperatures environment application. In order to achieve this, several sub-objectives are withdrawn:

- i. To develop nanostructured FeCr alloys by using spark plasma sintering method in order to reduce and control the grain growth of alloys.
- ii. To investigate the different sintering process, SPS and HP, in improving thermal stability of nanostructured FeCr alloy in terms of properties: thermal expansion, oxidation behaviour and electrical resistance.

- iii. To determine the effect of lanthanum ion implantation on the FeCr alloys microstructure and oxidation behaviour at 900, 1000 and 1100°C.
- iv. To compare the as developed FeCr alloy with the commercial alloy in terms of the investigated properties.
- v. To obtain the best method of developing novel FeCr based alloy for high temperature application, specifically interconnector SOFC material, based on the results analyzed.

#### 1.4 Scopes of Study

The scopes of this research include the following aspects:

- i. Development of nanostructured FeCr alloys by using SPS sintering method and compared with conventional HP sintering process.
- ii. Surface treatment via ion implantation with doses of lanthanum ion of  $1 \times 10^{17}$  ions/cm<sup>2</sup>.
- iii. Thermal expansion test by using push rod dilatometer-thermo mechanical analyzer between room temperature and 900 °C.
- iv. Cyclic oxidation test at 900, 1000 and 1100 °C for 100-hours oxidation times.
- v. Electrical resistance test of the oxidized sample by using the two point probe method.
- vi. Microstructure and phase analysis before and after the implementation of ion implantation and cyclic oxidation by using Scanning Electron Microscope (SEM), Energy Dispersion X-ray Spectroscopy (EDS), and X-Ray Diffraction analysis (XRD).
- vii. Determination of the optimum way of developing FeCr based alloy with and without lanthanum ion implantation and different consolidation technique for high temperature application as fuel cell interconnector based on the results analyzed.

## CHAPTER 2

### LITERATURE REVIEW

#### 2.1 Solid Oxide Fuel Cell

Solid oxide fuel cells (SOFC) are devices that generate electricity from the electrochemical conversion of a fuel and oxidant (Minh, 1993). A simplified configuration and operating principle of an SOFC using hydrogen as fuel is shown in Figure 2.1. A basic fuel cell comprised of three components: an electrolyte sandwiched between two electrodes (an anode and cathode). Under operating conditions, fuel enters and is oxidized at the anode portion of the cell, liberating electrons. Electrical power is produced as electrons flow from the anode to the cathode. Oxidant on the cathode side accepts electrons and is reduced to an ionic species. The circuit is completed by the diffusion of oxidant ions through the electrolyte. In practice fuel cells are not used individually, but in modular stacks where a fourth component—an electrical interconnect joins the individual cells. Since the reactants are often in the gaseous state, the interconnect usually serves to separate fuel and oxidant as well, thus preventing the fuel and oxidant gases from mixing. The interconnect is sometimes designated the bipolar plate, or separator, emphasizing the different polarities of anode and cathode which it connects or the gas separation, respectively.

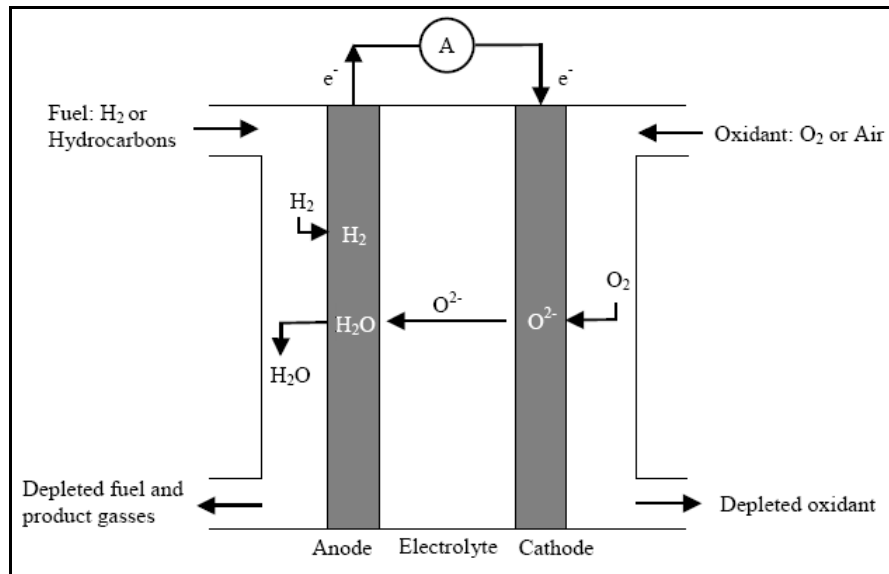


Figure 2.1: Typical SOFC single cell configuration (Minh, 1993)

For basic hydrogen SOFC, the electrochemical reactions involved are shown below (Minh, 1993):



Since the energy stored in the fuel is converted electrochemically and not through combustion, it is not subject to Carnot cycle limitations, so the energetic efficiency of a fuel cell is significantly higher (~60%) (Singhal, 2003; Steele, 2001). If the heat produced by the fuel cell is recaptured, efficiencies can reach ~80%. Fuel cells also produce much less polluting by products than traditional combustion processes. Additional advantages of fuel cells previously mentioned include their modular construction and potential for cogeneration of energy (electrical and thermal) (Minh, 1993).

The fuel and oxidant could, in theory, be any combination of gases that would provide the electrochemical reaction required for power generation to occur. Hydrogen is by far the most common fuel in use. The hydrogen can be in the form

of pure hydrogen gas, methane, or alcohols. The oxidant most commonly used is oxygen which is introduced into the SOFC in the form of natural air or as a pure gas. With these common gases, the fuel cell reaction produces by-products of water vapour and heat.

The flat-plate or planar type of SOFC has been the subject of intense research due to its potential for becoming an efficient, high energy-density power generation device. A schematic of a planar SOFC (Linderoth, Hendriksen, Mogensen & Langvad, 1996) is shown in Figure 2.2. The structure is comprised of individual layers of anode, electrolyte, cathode, and interconnect materials. The power capacity of a single cell is limited. The individual cells can be layered, or stacked, to form multi-cell structures thereby providing a higher voltage and power generation capabilities. Therefore, the structure requires a current collector between different cells to provide a higher voltage and power which provided by the interconnect.

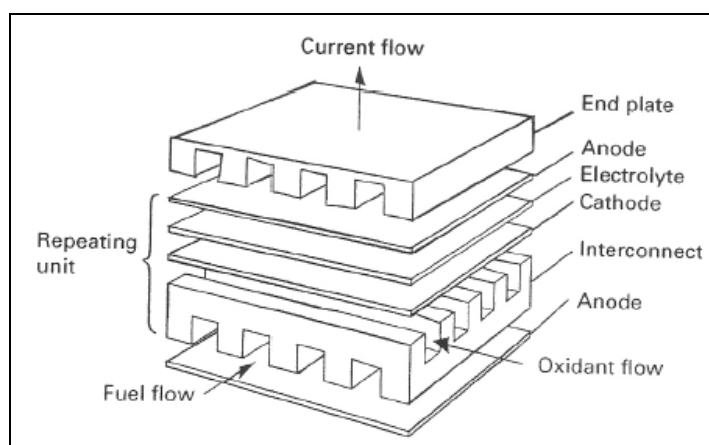


Figure 2.2: Schematic of a typical planar SOFC stack (Linderoth *et al.*, 1996)

## 2.2 Interconnect

The interconnect is the most complex of the four fuel cell components. The interconnect serves several vital functions in the SOFC structure. First, it provides electrical contact between cells allowing the stack to function as a single power generation unit. In addition, the interconnect keeps the oxidant and fuel gases from



mixing by forming a dense, physical barrier between the repeating cells. In certain designs, the interconnect may also provide mechanical support to the SOFC structure. The availability of a suitable material for the interconnect is of key importance for SOFC development.

The traditional material used for the SOFC interconnect is lanthanum chromites ( $\text{LaCrO}_3$ ). This material exhibits a remarkable high electric conductivity under SOFC operating conditions (Minh, 1993). Lanthanum chromites meet most of the above requirements and have proven to be suitable for conventional ceramic fuel cells. However the largest drawbacks for these materials are their high cost and poor sintering behaviour, which prevents their gas tightness (Minh, 1993). Also,  $\text{LaCrO}_3$  is ceramic, processing methods are limited which results in limitations as to the geometry of interconnect that can be fabricated. Because of these weaknesses of  $\text{LaCrO}_3$ , significant research efforts have been made to find an alternative material.

Metal alloys are widely seen as possessing superior properties compared with  $\text{LaCrO}_3$  which offer the potential to increase efficiency of the SOFC. Metals generally have very high electrical conductivity. Since any decrease in resistance of the cell would translate directly into increased output, moving to a more electrically conductive interconnect material could offer significant advantages. Thermal conductivity for metals is generally higher than for ceramics. Incorporating a high thermal conductivity material into a SOFC stack would serve to reduce temperature gradients within the structure that could impact thermal stresses and stack efficiency. Metals are generally easy to fabricate into a wide variety of shapes, which would allow designers to fabricate more complex SOFC designs. Also, many metals and alloys are relatively inexpensive and readily available.

Metallic alloys, however, also bring several negatives along with these potential benefits. The two main negative aspects of metal alloys for SOFC interconnects are oxidation of the metal during operation and the potential for problems arising due to thermal expansion mismatch between the metal and other SOFC materials. In a broad sense, metals tend to have higher coefficient of thermal expansion (CTE) compared with ceramics. In terms of the SOFC, this can cause significant levels of stress to develop when temperature changes. Metals also tend to oxidize when exposed to the range of temperatures and atmospheres commonly seen during operation of a SOFC. Excessive oxidation could lead to such problems as

reduced efficiency due to higher surface resistance of the interconnect layer. A discussion of potential interconnect alloys is given later in this section.

In general terms, the properties which a metal interconnect should possess can be described as follows (Quadackers *et al.*, 2003; Zhu & Deevi, 2003a):

- i) Thermal expansion. The thermal expansion of the interconnect metal should match with the other materials in the SOFC. It is particularly important that the alloy match well with the electrolyte, around  $10.5 \times 10^{-6}/^{\circ}\text{C}$ , so that the thermal stress developed during start-up and shut-down could be minimized.
- ii) Oxidation resistance. The alloy must not corrode severely under the operating conditions of the fuel cell in both anode and cathode atmospheres. The parabolic rate constant value for interconnect material is required below  $10^{-14} \text{ g}^2 \text{ cm}^{-4} \text{ s}^{-1}$ , and a value below  $10^{-15} \text{ g}^2 \text{ cm}^{-4} \text{ s}^{-1}$  would be ideal. Furthermore, the oxidation layer of the interconnect should exhibit some degree of electrical conductivity and should be adherent to the base alloy.
- iii) Electrical conductivity. The acceptable area-specific resistances (ASR) value for interconnect material is considered to be below  $100 \text{ m}\Omega\text{cm}^2$ .
- iv) Thermodynamic stability. The alloy must be thermodynamically stable during processing and operation of the SOFC. Because, the interconnect is exposed to both oxidizing conditions at the cathode and reducing conditions at the anode.
- v) Innocuous to other SOFC materials. The alloy and its oxidation layer should not contribute to the chemical degradation of other SOFC materials (i.e. chromia poisoning of the electrode).

For all these reasons, the interconnect materials constitute one of the basic components for the functioning and long term reliability SOFC operation stacks.

### 2.3 Potential Interconnect Alloys

Nowadays, interconnect-concept has been developed using metallic alloys. The majority of alloys currently investigated for fuel cell interconnects are comprised of various binary and ternary compositions, such as Cr-based or Fe-Cr binary alloys and

Fe-Ni-Cr ternary system. Using these types of materials has the advantage of their lower costs, easy fabrication and machinability and higher thermal conductivity in comparison with ceramic interconnects. Nevertheless, metallic alloys show the problem of a large CTE mismatch than that of the ceramic component, causing large stresses during cell operation. However, one of the most important features using these materials is that they are able to form protective oxides at the operating temperature. The formation of these oxides is of vital importance due to properties like electrical conductivity that shows a large dependence on them. An example can be found when an alumina forming alloy is used as interconnect. With such alloys and at the operating temperature, a very protective alumina oxide layer is formed on top of the surface, but the main inconvenience is that aluminium oxide has a very low electrical conductivity ( $10^{-6}$ - $10^{-8}$  Scm<sup>-1</sup> at 900 °C) compared with other oxides, specifically chromium oxide ( $10^{-2}$ - $10^{-1}$  Scm<sup>-1</sup> at 900 °C) (Zhu & Deevi, 2003a; Fergus, 2005). For this reason, the majority of interconnect alloy candidate researched are chromia formers (Yang *et al.*, 2003).

A metal interconnect must exhibit certain specific properties, several of which were outlined previously. Many materials can be immediately excluded from consideration based on these performance criteria and known material properties. For example, platinum would provide an excellent combination of oxidation resistance and electrical conductivity but the high material cost would be prohibitive for the economic production of these devices. Similarly, copper would be relatively inexpensive and highly conductive, but it would melt during the high-temperature processing of the hybrid stack. The following section provides an overview of potential alloy systems, highlighting recent work done and the potential each has for application as a SOFC interconnect. Several reviews on the topic of potential alloys for SOFC interconnects have been published recently (Linderoth *et al.*, 1996; Zhu & Deevi, 2003a; Quadackers *et al.*, 2003).

### 2.3.1 Iron-Chromium Alloys

The iron-chromium system has long been used as the basis of many engineering alloys for high-strength, corrosion-resistant applications. Chromium acts as an  $\alpha$ -

phase stabilizer when added to iron because chromium has the same body centre cubic (BCC) crystal structure as  $\alpha$ -iron. This results in the suppression of the face centre cubic (FCC)  $\gamma$ -phase of iron and creates the so-called " $\gamma$ -loop" in the Fe-Cr phase diagram, Figure 2.3 (ASM Handbook, 1992). At low temperatures, chromium and iron do not form a complete solid solution due to the presence of the  $\sigma$ -phase which has a tetragonal structure and is generally hard and brittle. The equilibrium phase diagram predicts the formation of  $\sigma$ -phase for alloys containing greater than 15 wt% Cr at temperatures between 475 and 821 °C. However, heat-treatments at high temperatures and long hold times or slow cooling rates are required for the formation of this phase. For a Fe 27 wt% Cr alloy, it was shown that the  $\sigma$ -phase would precipitate out of the  $\alpha$ -phase after holding at 565 °C for 131 days (Smith, 1993). A Fe-20 wt% Cr alloy, held at temperatures of 600 °C and above, would be within the  $\alpha$ -phase field and would therefore never form  $\sigma$ -phase even after extended high-temperature exposure.

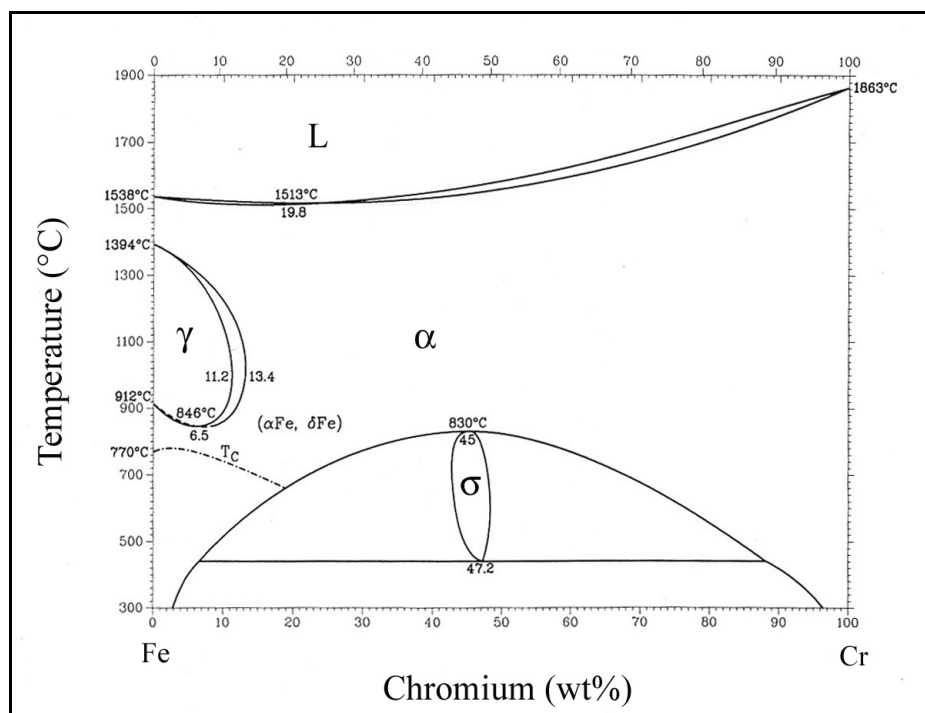


Figure 2.3: Phase diagram of Fe-Cr system (ASM Handbook, 1992)

Iron-chromium based alloys have been widely investigated for application as interconnects in fuel cells (Linderoth *et al.*, 1996; Huang, Hou & Goodenough, 2000;

Horita *et al.*, 2003a; Mullenberg *et al.*, 2003). Fe-Cr alloys containing between 15 and 40 wt% Cr have been shown to have average CTE values close to that of YSZ (Linderoth *et al.*, 1996). Oxidation rates of Fe-Cr alloys have been studied at SOFC operating temperatures in air (Linderoth *et al.*, 1996), wet air, (Mikkelsen & Linderoth, 2003), and carbon-containing (Horita *et al.*, 2003b) atmospheres.

Linderoth *et al.* (1996) used commercially provided binary Fe-Cr alloys ranging in composition from 10 to 60 wt% Cr to study thermal expansion and oxidation in air. It was shown that the best corrosion resistance was observed from a Fe 20 wt% Cr sample. The application of a ceria coating on the surface of a bare Fe 40 wt% Cr sample decreased the scale growth at 1000 °C in air by a factor of four compared with the same alloy without the ceria coating.

Uehara *et al.* (2003) investigated the impact of small alloying additions to Fe-Cr alloys containing ~ 20 wt% Cr on the oxidation rate and contact resistance of the oxide scale. Contact resistance was found to increase with chromium content while oxidation rate decreased with increasing chromium. The impact of small variations in Mn, Si, C, and Al additions were not significant in comparison to that due to a variation in chromium content.

Oxidation of a Fe 22 wt% Cr alloy was studied in wet air and hydrogen at two water vapour levels by Mikkelsen & Linderoth (2003). It was determined that a variation in the water vapour content in the oxidizing atmosphere affected oxidation rate; lower oxidation rates were observed with increased water vapour contents. This was determined to be due to the fact that wet air facilitated the vaporization of the chromia from the oxide layer, thereby lowering the observed weight gain of the sample. In addition, the oxide scale structure was observed to be different for oxides grown in hydrogen-rich or air atmospheres. Generally, the corrosion/oxidation resistance is maintained even at high temperature. They are particularly suitable for applications in aggressive and corrosive environments up to 900°C.

Horita *et al.* (2003b) studied the oxidation of two commercial Fe-Cr alloys containing 16 and 22 wt% Cr in a wet methane atmosphere at 800 °C. Results indicated that a higher chromium-containing alloy would have a slightly lower oxidation rate in that environment. Electrical conductivity measurements showed that the 22 wt% Cr alloy had higher conductivity after the oxidation experiment compared with the 16 wt% Cr alloy. The oxide layers for both alloys were found to be comprised of Cr<sub>2</sub>O<sub>3</sub> along with Fe-Mn-Cr spinel.

Additions of rare-earth elements, specifically Neodymium (Nd) and Praseodymium (Pr), were shown by Villafañe *et al.* (2003) to improve the oxidation resistance of a Fe-Cr alloy in air. Small additions of these elements (~ 0.03 wt%) were shown to drastically reduce weight gain of Fe 13wt% Cr alloy in air at 800 °C. It was shown by Ramanathan (1998) that the additions of small amounts of certain rare earth elements (Y, La) have been well documented in improving the oxidation protection properties of chromium.

The majority of researches conducted on Fe-Cr based alloys have used commercially available or supplier-provided experimental alloys. Oxidation behaviour of the alloy has typically been the main emphasis of research programs and only passing attention has been given to thermal expansion behaviour and other properties, such as electrical resistance. When thermal expansion has been investigated specifically, the published results have not been sufficiently detailed to allow for an exacting comparison of thermal expansion mismatch between the metal and electrolyte material. Presenting data in the form of  $\alpha$  versus temperature allows for a more complete picture of the material's behaviour. Therefore, Fe-Cr binary alloys were developed in the present work from the perspective of finding an alloy with sufficient properties of oxidation resistance, high-temperature electrical resistance and thermal expansion.

### 2.3.2 Other Metallic Materials

Other categories of chromia forming alloys including Ni(-Fe)-Cr base and Fe(-Ni)-Cr base alloys (e.g., austenitic stainless steels) have a FCC substrate structure. In comparison to the ferritic stainless steel (FSS), the FCC base alloys, in particular the Ni(-Fe)-Cr base alloys, are generally much stronger and potentially more oxidation resistant in the SOFC interconnect operating environment (Fergus, 2005; Linderoth *et al.*, 1996; Yang *et al.*, 2006a). However, the FCC Ni(-Fe)-Cr base alloys with sufficient Cr for an appropriate oxidation resistance often exhibit a high CTE, typically in the range of  $15.0$  to  $20.0 \times 10^{-6}/^{\circ}\text{C}$  from room temperature to 800 °C, and are much more expensive than the FSS. Due to the CTE mismatch, significant power loss or degradation in performance has been observed during

thermal cycling test of stacks using Ni(-Fe)-Cr base alloy interconnects (Wu & Liu, 2010).

The binary Fe-Ni alloys are generally not considered since this system fails to produce an adherent and protective oxide layer. The oxides of iron (FeO, Fe<sub>2</sub>O<sub>3</sub>, and Fe<sub>3</sub>O<sub>4</sub>) form non-uniform layers that spall under fuel cell condition. NiO similarly does little to impede diffusion and protect the alloy. Due to these reasons, little attention has been paid to this system for interconnects.

Nevertheless, Ni(-Fe)-Cr base alloys may find application as interconnect materials through the use of innovative SOFC stack and seal designs and novel interconnect structures. For example, a cladding approach has been applied to fabricate a stable composite interconnect structure consisting of FCC Ni-Cr base alloy claddings on a BCC FSS substrate (Chen, *et al.*, 2005a; Chen *et al.*, 2006). The clad structure appeared to be stable over 1000 hours at 800°C in air and exhibited a linear CTE close to that of the FSS, but needs further long-term stability evaluation before its commercial use.

Nickel-chromium alloys have not received significant attention as potential SOFC interconnect alloys (Yang, *et al.*, 2003) a notable exception generally because of the high CTE values observed in this system. In addition, these alloys are generally more expensive than other oxidation-resistant alloys due to the high nickel contents.

Traditional alloy design emphasizes surface and structural stability, but not the electrical conductivity of the scale formed during oxidation. In SOFC interconnect applications; the oxidation scale is part of the electrical circuit, so its conductivity is important. Thus, alloying practices used in the past may not be fully compatible with high-scale electrical conductivity. For example, Si, often a residual element in alloy substrates, leads to formation of a silica sublayer between scale and metal substrate. Immiscible with chromia and electrically insulating (Kofstad, 1983), the silica sublayer would increase electrical resistance, in particular if the subscale is continuous.

## 2.4 Consolidation Processing Route

It is well-known that materials with the same nominal composition can be produced in different ways, from classical melting and casting, practiced by conventional metallurgy, via powder consolidation by powder metallurgy methods, combustion synthesis with thermo-mechanical treatment, etc. Each technological route produces material having different microstructure, different concentrations and types of defects and therefore totally different properties. The first step in obtaining high-performance metal with a homogeneous microstructure and controlled grain size that meet the requirements of SOFC application is to prepare powders metal with controlled stoichiometry and small particle size. However, even if a small-size powder is used, conventional sintering is often unable to provide dense, very fine-grained metal, due to the high temperatures still required for densification.

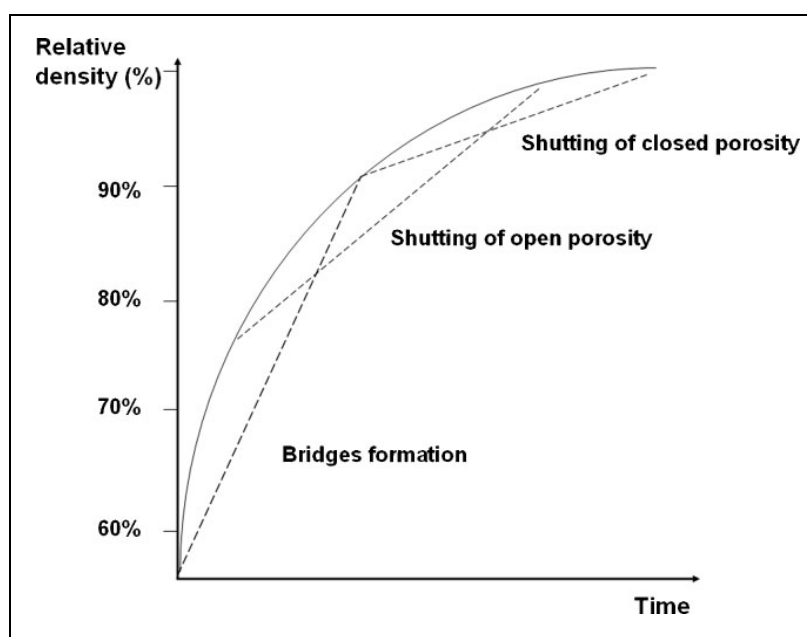


Figure 2.4: The three steps of sintering (Assollant, 1993; Kang, 2005)

In solid phase sintering (Figure 2.4), the temperature of the thermal treatment is slightly above two-thirds of the melting point. Sintering is subject of many influences: powder characteristics (morphology, dimension of the grains, purity, etc.), treatment (temperature, pressure, holding time) and atmosphere (vacuum,



reducing, oxidizing or inert (Ar, N<sub>2</sub>). The sintering process of the solid sample is considered to be thermodynamically irreversible. It is expressed by a lessening of the surface energy (free surface of the grains, then surfaces of the open and closed pores). Three steps are defined during the sintering (Assollant, 1993; Kang, 2005):

- i) Formation of a zone of connection between grains, called the bridge or neck of matter. This phenomenon is activated by diffusion mechanisms, evaporation-condensation, plastic deformation, etc., and ends when the bridges have been raised by close to 50% of the grain radii. This step is accompanied by an increase of ~15% of the density.
- ii) Elimination of the residual cavities or pores, the size of which is directly related to the surface energy. Being inter-connected, they form a continuous porosity, which diminishes and drives to a compactness of around 90%. Some cavities being instable will lead to some isolated pores.
- iii) The final step corresponds to almost full disappearance of the porosity, giving a fully dense material. Note that the grains tend to grow in this last step.

To take the advantage of the unique properties of the high performance nanostructured material the nanometer range powder particles have to be consolidated nearer to full theoretical density of the material, i.e. after consolidation nanostructures should be retained in the densified material. To achieve this it has to restrict the grain growth or coarsening during densification. Therefore, the temperature and time of consolidation are to be restricted at low value in order to achieve smaller grain sizes.

Among the methods reported for activation of the mass transport during the sintering process, the application of an electrical current through the sample during heating represents a promising technique for rapid densification of metal at relatively low temperatures. The most novel and increasingly used method is spark plasma sintering, which has clear advantages over conventional sintering methods, such as hot pressing, making it possible to sinter nanometric powder to near full densification with little grain growth.

This has become increasingly important recently, with the high thermal stability application in SOFC system and the need to investigate size effects on the properties in approaching the nanometer scale. Therefore, the two consolidation

methods are used for sintering Fe-Cr powder in this work: the SPS and the HP.

Figure 2.5 shows generally the powder metallurgy route which had been explored in this project.

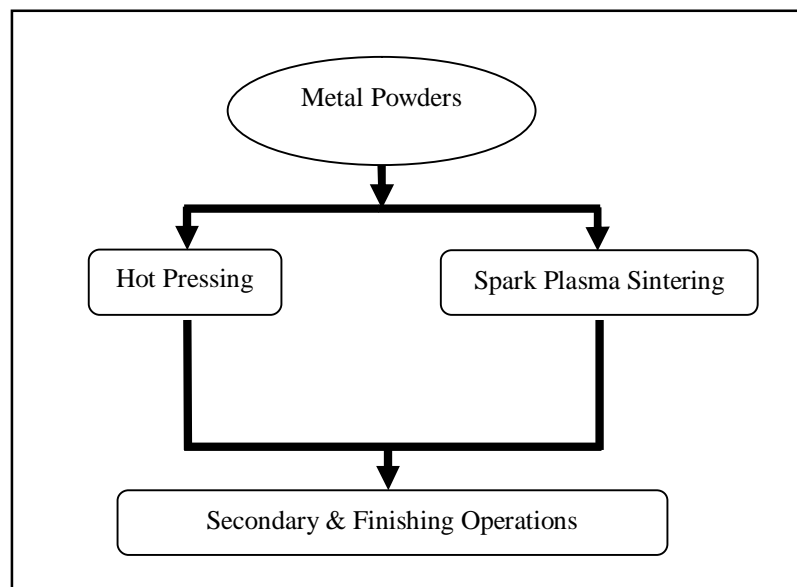


Figure 2.5: Powder metallurgy route

## 2.5 Sintering

Sintering is a process of using heat to turn powdered substances into solids without actually melting the material and is the most common technique for consolidating powders. During sintering, the pressed powder particles fuse together, forming metallurgical bonds. Essentially, it is the removal of the pores between the starting particles, combined with their growth and strong mutual bonding. The process is carried out by heating up the “green” part at about 70 to 80 % of the melting temperature, until full strength is obtained within several minutes to hours. The biggest problem of this technique is the shrinkage which causes cracking and distortion. There are many methods of sintering a component. The process is usually divided in four categories: solid-state sintering; liquid-phase sintering, viscous flow sintering; and transient liquid phase sintering. Overpressure sintering uses also pressure to accelerate densification. In this work, the mechanically alloyed

powders had been sintered in two different vacuum sintering methods: hot pressing and spark plasma sintering. The schematic of the hot pressing technique is shown in Figure 2.6, while Figure 2.7 shows the schematics of the structural changes accompanying the preparation of a sintered product.

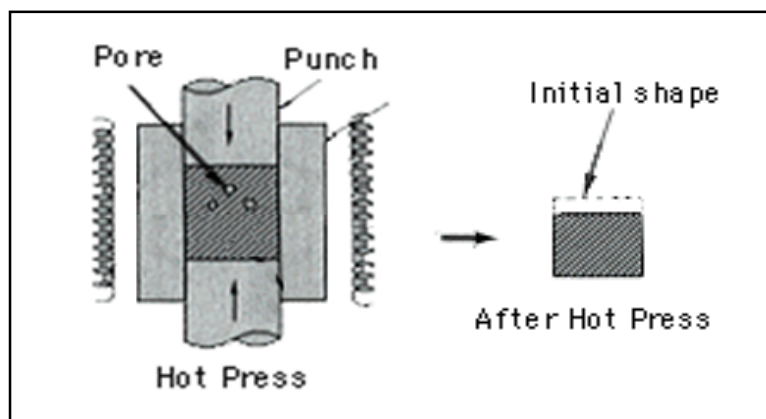


Figure 2.6: Schematic of the hot pressing technique (Ashby *et al.*, 2007)

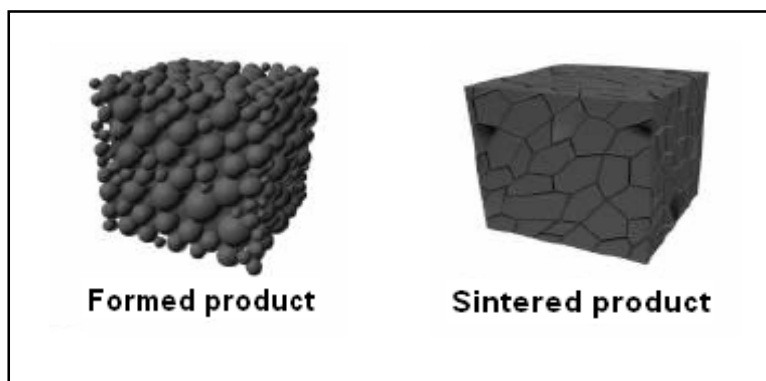


Figure 2.7: Structural changes accompanying the preparation of a sintered product (Ashby *et al.*, 2007)

The spark plasma sintering (SPS) technique is a fast and relatively new alternative to conventional hot pressing (HP) used for solidification. Several different materials can be compacted by the SPS technique: metals, composites, and oxides, nitrates, carbides, mesoporous materials, etc. Even materials which are considered to be difficult to sinter can be sintered in short times and at relatively low temperatures to full density. SPS has also recently been used to sinter carbon nanotubes with copper (Daoush, 2008; Daoush *et al.*, 2009).

The SPS configuration is similar to the conventional HP setup. In both cases the precursor powder (green body) is loaded into a die, usually made of graphite, and a uniaxial pressure is applied during sintering process to solidify the powder. In the HP unit the die is heated by heating elements located in the reaction chamber. In SPS unit there is no external heating element but the die is heated by a pulsed DC current that goes through the conductive die, i.e. the die serves both as pressure die and heating element. This means that the sample can be heated from both outside and inside. The use of a pulsed direct current also implies that the samples are exposed to a pulsed electric field during the sintering process.

The SPS technique resembles HP to a great extent as discussed below. The benefits of the SPS technique compared to the HP technique can be summarized as: (i) Rapid heating/cooling rates and short sintering times can be applied; (ii) Higher pressures can be used, which in turn yields higher densities at lower temperatures; (iii) The presence of an electric current/field is said to enhance/activate the sintering; (iv) Most materials can be densified at low temperatures using considerably shorter sintering times.

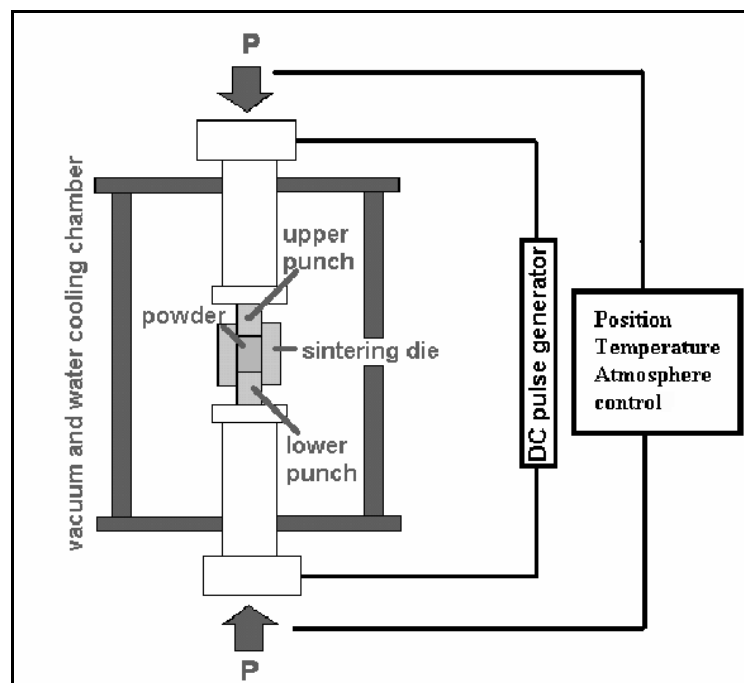


Figure 2.8: Basic configuration of a typical SPS system (Tokita, 2006)

The basic configuration of a SPS unit is shown in Figure 2.8. It consists of a uniaxial pressure device, where the water-cooled punches also serve as electrodes, a water-cooled reaction chamber that can be evacuated, a pulsed direct current (DC) generator and pressure-, position- and temperature-regulating systems. In an SPS experiment, a weighed amount of powder is introduced in a die. The die may be built up with various materials, such as carbon, WC, refractory alloys, etc.

SPS is a pressure-assisted sintering method that is thought to be based on momentary high-temperature spark (and/or plasma, if present) discharges in the gaps between powder particles at the beginning of the ON-OFF DC current pulses. It is supposed that the pulsed current propagates through the powder particles inside the SPS sintering die, as shown in Figure 2.9. The process inventor also claims that the ON- OFF DC pulse energising method generates: (i) Spark plasma; (ii) Spark impact pressure; (iii) Joule heating; and (iv) An electrical field promoting material transfer and diffusion (Tokita, 2000; Tokita 2002; Tokita, 2006).

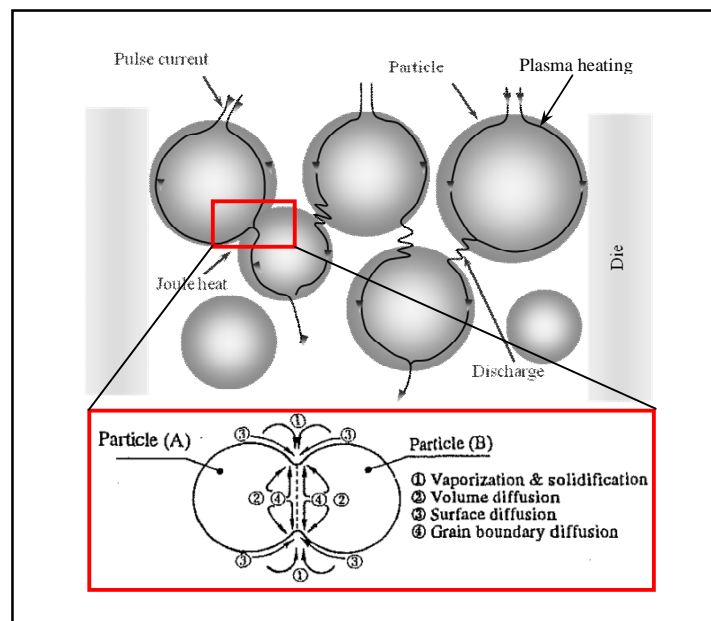


Figure 2.9: A schematic drawing of the pulsed current that flows through powder particles (Tokita, 2006)

The major interest in this process, when the sintering parameters have been mastered, is linked to the extreme rapidity of the thermal treatment. Thus, the consolidation time is greatly decreased from hours, in the case of the conventional

sintering, to few minutes for the SPS process. Moreover, the sintering temperature can be diminished by a few hundred degrees compared to conventional hot pressing sintering.

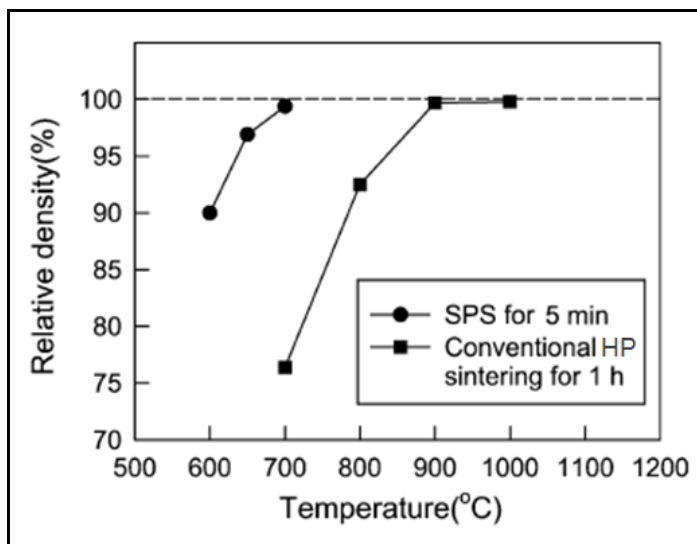


Figure 2.10: Comparison of the relative densities of the Ti specimen prepared by SPS and conventional HP sintering as a function of the sintering temperature (Eriksson, 2007)

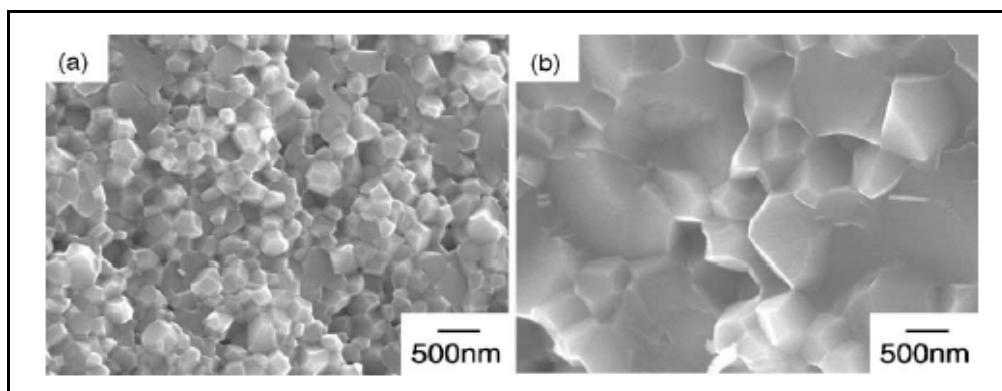


Figure 2.11: SEM fractured surfaces of the Ti specimen prepared (a) by SPS at 700 °C for 5 min and (b) by conventional HP sintering at 900 °C for 1 h (Eriksson, 2007)

It was shown by Eriksson (2007) that the densification takes place significantly much faster in the SPS than that in HP process. Figure 2.10 shows two typical relative density-temperature profiles used in SPS and HP process, yielding fully densified Ti specimen with different microstructures. SEM pictures of these

samples are shown in Figure 2.11. The average grain size was noticeably different depending on the sintering method, as shown in SEM micrograph (Figure 2.11). In conventional HP sintering, the specimen was fully densified after sintering at temperatures above 900 °C for 1 h. In contrast, when the samples were prepared by SPS, the relative density of the theoretical value was reached 99% at 700 °C. Moreover, even 5 min of treatment using SPS at 600–700 °C resulted in a significantly high density (95 - 99%). A comparison of the two densification curves obtained from conventional HP sintering and SPS indicates that employing SPS is effective in obtaining fully-densified specimen with a minimum grain growth at a low sintering temperature by approximately 200 °C. This also shows that SPS constitutes an innovative technique in the field of material sintering and three distinguishing factors contribute to its enhanced densification compared to conventional HP process: i) DC current influence, ii) high heating rates, and, iii) the simultaneous application of pressure.

## **2.6 Surface Treatments via Ion Implantation**

Thermal stability of the metallic interconnect can influence the efficiency of the stack such as the increased electrical resistance due to the growth of oxide layer. There are two general methods used to improve the thermal stability of an alloy; alloying addition and surface treatment such as by ion implantation. Of these two methods, only surface treatments – ion implantation are discussed here.

Ion Implantation is a physical method for the modification of surface properties of materials by insertion of accelerated atoms, within the first atomic layers into solid substrates. Ionized atoms are made to accelerate and to bombard the solid surface. As a consequence, there can be distinct modifications to near-surface microstructure and chemical, physical and mechanical properties which for example can appear as changes in corrosion behaviour, electrical properties, stiffness, hardness, wear resistance, friction response, or other surface-region-sensitive mechanical properties such as fatigue and contact fracture toughness. Nowadays, this technique is commonly employed for the surface treatment of cutting and

## REFERENCES

- Ailor, W.H. (1971). *Handbook of Corrosion Testing and Evaluation*. New York: John Wiley.
- Antepara, I., Villarreal, I., Rodríguez-Martínez, L. M., Lecanda, N., Castro, U., & Laresgoiti, A. (2005). Evaluation of ferritic steels use as interconnects and porous metal supports in IT-SOFCs. *J. Power Sources*, *151*, pp. 103 – 107.
- Ashby, M., Sherclif, H., & Cebon, D. (2007). *Materials: Engineering, Science, Processing and Design*. Oxford: Elsevier.
- ASM Handbook Vol. 3. (1992). Alloy Phase Diagrams. Materials Park, OH: ASM International.
- Assollant, D. B. (Ed) (1993). *Chimie-physique du frotage* (in English version). Paris: Hermes FORCERAM Collection.
- Benenson, W., Harris, J. W., Stocker, H., & Lutz, H. (2002). *Handbook of Physics*. New York: Springer-Verlag Inc.
- Bloor, Brook, Flemings, & Mahajan. (1994). *Ion Implantation*. The Encyclopedia of Advanced Material. Oxford: Pergamon.
- Chen, L., Yang, Z., Jha, B., Xia, G., & Stevenson, J. W. (2005a). Clad metals, roll bonding and their applications for SOFC interconnects. *J. Power Sources*, *152(1)*, pp. 40 – 45.



- Chen, L., Jha, B., Yang, Z., Xia, G., Stevenson, J. W., & Singh, P. (2006). Clad metals by roll bonding for SOFC interconnects. *J. Mater. Eng. Perform*, *15*(4), pp. 399 – 403.
- Chen, X., Hou, P. Y., Jacobson, C. P., Visco, S. J., & De Jonghe, L. C. (2005b). Protective coating on stainless steel interconnect for SOFCs: Oxidation kinetics and electrical properties, *Solid State Ionics*, *176*, pp. 425–433.
- Cooper, L., Benhaddad, S., Wood, A., & Ivey, D. G. (2008). The effect of surface treatment on the oxidation of ferritic stainless steel used for solid oxide fuel cell interconnects. *Journal of Power Sources*, *184*, pp. 220–228.
- Daoush, W. M. (2008). Processing and characterization of CNT/Cu nanocomposites by powder technology. *Powder Metallurgy and Metal Ceramics*, *47*(9/10), pp. 531 - 537.
- Daoush, W. M., Lim, B. K., Mo, C. B., Nam, D. H., & Hong, S. H. (2009). Electrical and mechanical properties of carbon nanotube reinforced copper nanocomposites fabricated by electroless deposition process. *Materials Science and Engineering: A*, *513-514*(C), pp. 247 - 253.
- Ding, W., Wang, X., Zeng, X., Wu, G., Yao, S., & Lai, Y. (2007). Cyclic oxidation behavior of Cerium implanted AZ31 magnesium alloys. *Materials Letters*, *61*, pp. 1429 – 1432.
- Dyos, G. T. & Farrel, T. (1992). *Electrical Resistivity Handbook*. London: Peter Peregrinus Ltd.
- Echsler, H., Martinez, E. A., Singheiser, L., & Quadackers, W. J. (2004). Residual stresses in alumina scales grown on different types of Fe–Cr–Al alloys: Effect of specimen geometry and cooling rate. *Materials Science and Engineering A*, *384*, pp. 1 – 11.

- Eriksson, M. (2007). *Spark Plasma Sintering and Deformation Behaviour of Titanium and Titanium/TiB<sub>2</sub> Composites*, Division of Inorganic Chemistry, Stockholm University: Licentiate Thesis.
- Essuman, E., Meier, G. H., Zurek, J., Hansel, M., Singheiser, L., & Quadackers, W. J. (2007). Enhanced internal oxidation as trigger for breakaway oxidation of Fe–Cr alloys in gases containing water vapor. *Scripta Materialia*, 57, pp. 845 – 848.
- Fergus, J. W. (2005). Metallic interconnects for solid oxide fuel cells. *Materials Science and Engineering A*, 397, pp. 271 – 283.
- Fernandes, S. M. D. C., & Ramanathan, L.V. (2007). Cyclic oxidation resistance of rare earth oxide gel coated Fe-20Cr alloys. *Materials Research*, 10(3), pp. 321 - 324.
- Filetin, T. (2001). *An Overview of the Development and Application of Advanced Materials*. Zagreb: Croatian Welding Society.
- Fontana, M. G. (1986). *Corrosion Engineering*. 3<sup>rd</sup> ed. International Student Edition. New York: McGraw-Hill.
- Fontana, S., Amendola, R., Chevalier, S., Piccardo, P., Caboche, G., Viviani, M., Molins, R., & Sennour, M. (2007). Metallic interconnects for SOFC: Characterisation of corrosion resistance and conductivity evaluation at operating temperature of differently coated alloys. *Journal of Power Sources*, 171, pp. 652 – 662.
- Gao, W. & Li, Z. (2004). Nano-structured alloy and composite coatings for high temperature applications. *Material Research*, 7(1), pp. 175-182.
- Gupta, R. K., Singh Raman, R. K., & Koch, C. C. (2010). Fabrication and oxidation resistance of nanocrystalline Fe<sub>10</sub>Cr alloy. *J. Mater. Sci.*, 45, pp. 4884–4888.

- Horita, T., Xiong, Y., Yamaji, K., Sakai, N., & Yokokawa, H. (2003a). Characterization of Fe-Cr alloys for reduced operation temperature SOFCs. *Journal of the Electrochemical Society*, 2, pp. 189-194.
- Horita, T., Xiong, Y., Yamaji, K., Sakai, N., & Yokokawa, H. (2003b). Stability of Fe-Cr alloy interconnects under CH<sub>4</sub>-H<sub>2</sub>O atmosphere for SOFCs. *Journal of Power Sources*, 118(1), pp.35-43.
- Huang, K., Hou, P. Y., & Goodenough, J. B. (2000). Characterization of iron-based alloy interconnects for reduced temperature solid oxide fuel cells. *Solid State Ionics*, 129(1), pp. 237 - 250.
- Kang, S. J. L. (2005). *Sintering: Densification, Grain Growth, and Microstructure*. Oxford: Elsevier.
- Kofstad, P. (1983). *Nonstoichiometry, Diffusion, and Electrical Conductivity in Binary Metal Oxides*. Florida: Robert E. Krieger Publishing Company.
- Kofstad, P. (1988). *High Temperature Corrosion*. New York: Elsevier Applied Science.
- Kuru, Y., Wohlschlogel, M., Welzel, U., & Mittemeijer, E. J. (2007). Crystallite size dependence of the coefficient of thermal expansion of metals. *Applied Physics Letters*, 90, pp. 243113-1 – 243113-3.
- Larsen, P. H., Hendriksen, P. V., & Mogensen, M. (1997). Dimensional stability and defect chemistry of doped lanthanum chromites. *J. Thermal Analysis*, 49, pp. 1263 – 1275.
- Li, M.-S., Qian, Y.-H., & Zhou, Y.-C. (2008). Oxidation of pre-oxidized GH128 alloy implanted with Ce<sup>+</sup> at 1000 °C. *Trans. Nonferrous Met. Soc. China*, 18, pp. 493 – 498.

- Linderoth, S., Hendriksen, P.V., Mogensen, M., & Langvad, N. (1996). Investigations of metallic alloys for use as interconnects in solid oxide fuel cell stacks. *Journal of Materials Science*, 31, pp. 5077 - 5082.
- Marest, G. (1998). Surface treatment by ion implantation. *Hyperfine Interactions*, 111, pp. 121 -127.
- Minh, N.Q. (1993). Ceramic fuel cells. *Journal of the American Ceramic Society*, 76(3), pp. 563 - 588.
- Mullenberg, W. A. Uhlenbruck, S., Wessel, E., Buchkremer, H. P., & Stover, D. (2003). Oxidation behaviour of ferrous alloys used as interconnecting material in solid oxide fuel cells. *Journal of Materials Science*, 38, pp. 507.
- Mikkelsen, L. & Linderoth, S. (2003). High temperature oxidation of Fe-Cr alloy in O<sub>2</sub>-H<sub>2</sub>-H<sub>2</sub>O atmospheres; microstructure and kinetics. *Materials Science and Engineering A*, 361, pp.198 - 212.
- Monceau, D. & Pieraggi, B. (1998). Determination of parabolic rate constants from a local analysis of mass-gain curves. *Oxidation of Metals*, 50(5/6), pp. 477-493.
- Omori, M. (2000). Sintering, consolidation, reaction and crystal growth by the spark plasma system (SPS). *Material Science and Engineering A*, 287, pp. 183 - 188.
- Peng, H. (2004). *Spark Plasma Sintering of Si<sub>3</sub>N<sub>4</sub>-Based Ceramics: Sintering Mechanism-Tailoring Microstructure-Evaluating Properties*, Department of Inorganic Chemistry, Stockholm University: Ph.D Thesis.
- Pilis, M. F. & Ramanathan, L. V. (2007). High temperature oxidation resistance of rare earth chromite coated Fe-20Cr and Fe-20Cr-4Al alloys. *Materials Research*, 10(3), pp. 279 – 282.

- Quadackers, W.J., Abellan, J. P., Shemet, V., & Singheiser, L. (2003). Metallic interconnectors for solid oxide fuel cells – a review. *Materials at High Temperatures*, 20(2), pp. 115 - 127.
- Ramanathan, L. V. (1998). Corrosion control with rare earths. *Corrosion Prevention and Control*, 45(3), pp. 87 - 92.
- Riffard, F., Buscail, H., Caudron, E., Cueff, R., Issartel, C., & Perrier, S. (2006). The influence of implanted Yttrium on the cyclic oxidation Behaviour of 304 Stainless Steel. *Applied Surface Science*, 252, pp. 3697 – 3706.
- Saryanto, H. (2011). *High Temperature Oxidation Resistance of Nanocrystalline Fe<sub>80</sub>Cr<sub>20</sub> Alloys and Ferritic Steel Implanted with Lanthanum and Titanium*, Faculty of Mechanical and Manufacturing Engineering, Universiti Tun Hussein Onn Malaysia: Master Thesis.
- Sebayang, D., Khaerudini, D. S. Saryanto, H., Othman, M. A. Sujitno, T., & Untoro, P. (2011). Effect of nanocrystalline and Ti implantation on the oxidation behaviour of Fe<sub>80</sub>Cr<sub>20</sub> alloy and commercial ferritic steel. *Key Engineering Materials*, 474-476, pp. 2134-2139.
- Shaigan, N., Qu, W., Ivey, D. G., & Chen, W. (2010). A review of recent progress in coatings, surface modifications and alloy developments for solid oxide fuel cell ferritic stainless steel interconnects. *Journal of Power Sources*, 195, pp. 1529 - 1542.
- Shiratori, Y., Tietz, F., Buchkremer, H. P., & Stover, D. (2003). YSZ–MgO composite electrolyte with adjusted thermal expansion coefficient to other SOFC components. *Solid State Ionics*, 164, pp. 27–33.
- Singhal, S. (2003). Ceramic fuel cells for stationary and mobile applications. *American Ceramic Society Bulletin*, pp. 9601 - 9610.

- Smith, W. F. (1993). *Structure and Properties of Engineering Alloys*. 2<sup>nd</sup> ed. New York: McGraw-Hill.
- Smith, W. F. (1996). *Principles of Materials Science and Engineering*. New York: Mc Graw-Hill.
- Steele, B. C .H. (2001). Material science and engineering: The enabling technology for the commercialisation of fuel cell systems. *Journal of Materials Science*, 36, pp. 1053 - 1068.
- Stöver, D., Diekmann, U., Flesch, U., Kabs, H., Quadackers, W. J., Tietz, F., & Vinke, I. (1999). Recent developments in anode supported thin film SOFC at Research Centre Jülich. *Proceedings 6<sup>th</sup> International Symposium Solid Oxide Fuel Cells (SOFC-VI)*, Pennington, NJ, The Electrochemical Society, pp. 812 - 821.
- Suryanarayana, C. (2004). *Mechanical Alloying and Milling*. New York: Marcel Dekker.
- Taylor, R. E. (1998). *Thermal Expansion of Solids*. Ohio: ASM International.
- Tietz, F., Buchkremer, H. -P., & Stöver, D. (2002). Components manufacturing for solid oxide fuel cells. *Solid State Ionics*, 152-153, pp. 373 – 381.
- Tietz, F. (1999). Thermal expansion of SOFC materials. *Ionics*, 5, pp. 129 - 139.
- Tokita, M. (2000). Current status of spark plasma sintering. *Sokeizai*, 41, pp. 8 - 13.
- Tokita, M. (2002). Spark plasma sintering apparatus. *Nanoryushi no Seizo-Hyoka-Oyo-Kiki no Saishin Gijutsu*, pp. 146-153.
- Tokita, M. (2006). Innovative sintering process-spark plasma sintering (SPS). *Materials Integration*, 19(12), pp. 42 - 50.

- Uehara, T., Toji, A., Inoue, K., Yamaguchi, M., & Ohno, T. (2003). *Solid Oxide Fuel Cells VIII Proceedings of the International Symposium*, Pennington, N.J. The Electrochemical Society, pp. 915.
- Villafañe, A. M., Chacon-Nava, J. G. Gaona-Tiburcio, C., Calderon, F. A., Patiño, G. D., & Gonzalez-Rodriguez, J. G. (2003). Oxidation performance of a Fe-13Cr alloy with additions of rare earth elements. *Materials Science and Engineering A*, 363, pp. 15.
- Williamson, G. K. & Hall, W. H. (1953). X-ray line broadening from filed aluminium and wolfram. *Acta Metallurgica*, 1, pp. 22 – 31.
- Wu, J. & Liu, X. (2010). Recent development of SOFC metallic interconnect. *J. Mater. Sci. Technol.*, 26(4), pp. 293 – 305.
- Yang, Z. G., Weil K. S., Paxton, D. M., & Stevenson, J. W. (2003). Selection and evaluation of heat-resistant alloys for SOFC interconnect applications. *Journal of the Electrochemical Society*, 150(9), pp. A1188 - A1201.
- Yang, Z., Xia, G., Singh, P., & Stevenson, J.W. (2006a). Evaluation of Ni-Cr-base alloys for SOFC interconnect applications. *Journal of Power Sources*, 160(2), pp. 1104 – 1110.
- Yang, Z., Xia, G., Singh, P., & Stevenson, J.W. (2006b). Electrical contacts between cathodes and metallic interconnects in solid oxide fuel cells. *Journal of Power Sources*, 155, pp. 246 – 252.
- Young, D. (2008). *High Temperature Oxidation and Corrosion of Metals*. Amsterdam: Elsevier.
- Zhang, H. W., Gopalan, R., Mukai, T., & Hono, K. (2005). Fabrication of bulk nanocrystalline Fe–C alloy by spark plasma sintering of mechanically milled powder. *Scripta Materialia*, 53, pp. 863 – 868.

Zhu, W. Z. & Deevi, S. C. (2003a). Development of interconnect materials for solid oxide fuel cells. *Materials Science and Engineering A*, 348, pp. 227 - 243.

Zhu, W. Z. & Deevi, S. C. (2003b). Opportunity of metallic interconnects for solid oxide fuel cells: a status on contact resistance. *Materials Research Bulletin*, 38, pp. 957 – 972.